Journal of African Earth Sciences 129 (2017) 779–791

Contents lists available at ScienceDirect

Journal of African Earth Sciences

journal homepage: www.elsevier.com/locate/jafrearsci

Reservoir characterization and seal integrity of Jemir field in Niger Delta, Nigeria

Theophilus Aanuoluwa Adagunodo [a, *], Lukman Ayobami Sunmonu [a], Moruffdeen Adedapo Adabanija [b]

[a] Department of Pure and Applied Physics, Ladoke Akintola University of Technology, Ogbomoso, Nigeria
[b] Department of Earth Sciences, Ladoke Akintola University of Technology, Ogbomoso, Nigeria

ARTICLE INFO

Article history:
Received 19 April 2016
Received in revised form
9 February 2017
Accepted 10 February 2017
Available online 20 February 2017

Keywords:
Faults
Hydrocarbons
Niger delta
Reservoir characterization
Seal integrity
Structural traps

ABSTRACT

Ignoring fault seal and depending solely on reservoir parameters and estimated hydrocarbon contacts can lead to extremely unequal division of reserves especially in oil fields dominated by structural traps where faults play an important role in trapping of hydrocarbons. These faults may be sealing or as conduit to fluid flow. In this study; three-dimensional seismic and well log data has been used to characterize the reservoirs and investigate the seal integrity of fault plane trending NW-SE and dip towards south in Jemir field, Niger-Delta for enhanced oil recovery. The petrophysical and volumetric analysis of the six reservoirs that were mapped as well as structural interpretation of the faults were done both qualitatively and quantitatively. In order to know the sealing potential of individual hydrocarbon bearing sand, horizon–fault intersection was done, volume of shale was determined, thickness of individual bed was estimated, and quality control involving throw analysis was done. Shale Gouge Ratio (SGR) and Hydrocarbon Column Height (HCH) (supportable and structure-supported) were also determined to assess the seal integrity of the faults in Jemir field.

The petrophysical analysis indicated the porosity of traps on Jemir field ranged from 0.20 to 0.29 and the volumetric analyses showed that the Stock Tank Original Oil in Place varied between 5.5 and 173.4 Mbbl. The SGR ranged from leaking (<20%) to sealing (>60%) fault plane suggesting poor to moderate sealing. The supportable HCH of Jemir field ranged from 98.3 to 446.2 m while its Structure-supported HCH ranged from 12.1 to 101.7 m.

The porosities of Jemir field are good enough for hydrocarbon production as exemplified by its oil reserve estimates. However, improper sealing of the fault plane might enhance hydrocarbon leakage.

1. Introduction

Oil and gas resources sourced mainly from Niger Delta had accounted for 80% of the Nigerian government's revenue and 95% of the country's export earnings since 1970s. However, there have been some irregularities recorded in the recent time from the exploration and production companies in Niger Delta, such as dry wells or unbalanced record of oil reserves. Till date twenty-three oil fields have been shut in or abandoned as a result of poor prospectivity or total drying up of the wells (Oil and Gas, 2015). The need to thoroughly evaluate prospects so as to determine optimal production strategies and also minimize risk that may be associated with hydrocarbon exploration has driven the development of an array of techniques which attempt to propagate log properties (Formation evaluation). These include the use of deterministic and linear physical relationship between log properties and the corresponding seismic response of subsurface rock units (e.g. Muslime and Moses, 2011; Eshimokhai and Akhirevbulu, 2012) as well as reservoir characterization (Schlumberger, 1989; Eshimokhai and Akhirevbulu, 2012). However, sequel to estimation of petrophysical parameters and oil reserves in a field; it is paramount to analyze the sealing potential (seal integrity) of the fault supporting the trap in order to know whether the rock structure is capable to keep oil and gas from migrating out of the trap or not.

Seal integrity is the analysis of substance that forms barrier in

* Corresponding author.
E-mail addresses: taadagunodo@yahoo.com, taadagunodo@gmail.com, taadagunodo@pgschool.lautech.edu.ng (T.A. Adagunodo), lasunmonu@lautech.edu.ng (L.A. Sunmonu), maadabanija@lautech.edu.ng, tunde.adabanija@gmail.com (M.A. Adabanija).

http://dx.doi.org/10.1016/j.jafrearsci.2017.02.015
1464-343X/

fault. Fault plays an important role in creating hydrocarbon traps because it serves as house which hydrocarbon lives. Seals are fundamental (i.e. no seal no trap). Seals also control the movement of hydrocarbons during production. Faults that do not form seal may prevent oil and gas from accumulating in the subsurface. Open and permeable faults in reservoir may also cause serious lost-circulation problems during drilling operations (Oniyangi, 2008). Consequently, if fault leaks; they provide field-wide communication among numerous fault compartments. Thus, ignoring seal integrity of fault plane and depending solely on reservoir parameters and estimated hydrocarbon contacts can lead to extremely unequal division of reserves.

Reservoirs characterization have been done on many fields of Niger Delta (Eshimokhai and Akhirevbulu, 2012; Ameloko and Omali, 2013; Oyedele et al., 2013; Oyeyemi and Aizebeokhai, 2015) but few have been reported about seal integrity – a gap that is essential to be filled in order to enhance the recovery and improve the reserve portfolio. Hence the current study was aimed to characterize the reservoirs and investigate the seal integrity of reservoirs for enhanced oil recovery of Jemir field in Niger-Delta, Nigeria. The specific objectives of the study include identification of structural trap, estimation of petrophysical parameters and volume of hydrocarbon reserves, establishment of throw distribution across the interpreted fault-dependent structures, determination of Shale Gouge Ratio (SGR) and Hydrocarbon Column Height (HCH) (supportable and structure-supported). The determination of SGR is hinged on its suitability to predict the sealing capacity of faults (Yielding et al., 1997) as faults with sand-rich gouge tend to leak; whereas faults with shale-rich gouge tend to seal. The HCH will estimate the likely hydrocarbons' height that a fault can support because fault does not only control how much hydrocarbons are in a trap, but also the vertical distribution of hydrocarbons among a series of stacked sands.

2. Location and geology of the study area

Jemir field is an offshore field located in the western region of Niger Delta: one of the Nigerian sedimentary basins (Fig. 1). The field has total coverage of 113.2 km^2. The Niger-Delta which covers an area of about 75,000 sq km is situated in southern Nigeria between latitudes 4° N to 7° N and longitude 5° E to 8° E (Fig. 2). It is bounded to the west and northwest by the western African shield,

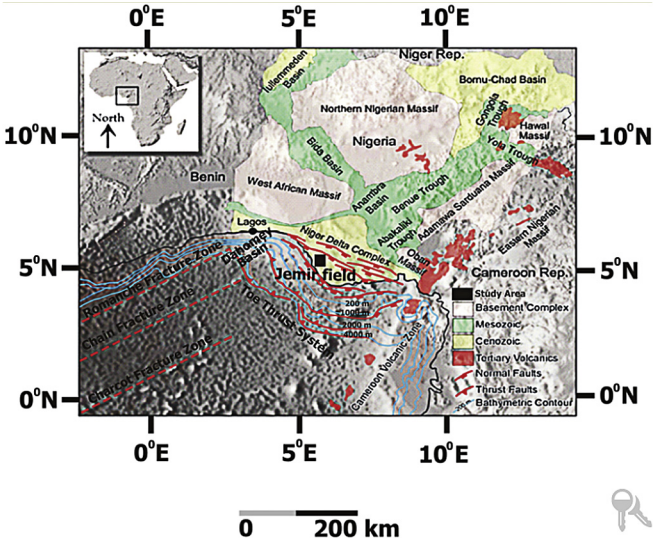

Fig. 1. Map of Niger-Delta showing the study area.

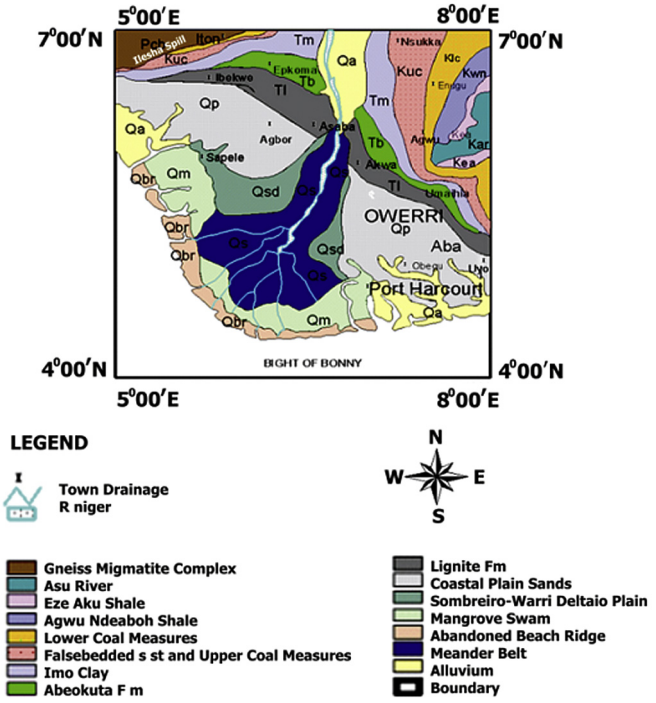

Fig. 2. Geological map of Niger-Delta (adapted from Amadi et al., 2012).

which terminates at the Benin hinge line; to the east by the Calabar hinge line; to the north by the Anambra basin and Abakaliki anticlinorium; and to the south by the gulf of Guinea (Oyedele et al., 2013). It extends in an East-West direction from South-West Cameroun to the Okiti-pupa Ridge with its apex situated south-east of the confluent of the Niger and Benue Rivers.

Jemir field is geologically concealed within Tertiary section of the Niger Delta comprising three Formations: Benin, Paralic Agbada and pro-delta Marine Akata Formation representing prograding depositional facies distinguished mostly on the basis of sand-shale ratio (Short and Stauble, 1967; Doust and Omatsola, 1990; Kulke, 1995; Ameloko and Omali, 2013). The Benin Formation is a continental latest Eocene to Recent deposit of alluvial and upper coastal plain sands. It consists predominantly freshwater baring massive continental sands and gavels deposited in an upper deltaic plain environment. The Agbada Formation consists paralic siliciclastics, which underlies the Benin Formation. It consists fluviomarine sands, siltstones and shales. The sandy parts constitute the main hydrocarbon reservoirs. The grain size of these reservoir ranges from very coarse to fine. The Akata Formation is the basal unit of the Tertiary Niger Delta complex. It is of marine origin and composed of thick shale sequence (potential source rock), turbidite sands (potential reservoirs in deep water) and minor amount of clay and silt.

Doust and Omatsola (1989) documented that normal faults activated by the movement of deep seated, ductile, overpressured marine shale have marred greatly the Niger Delta clastic wedge. Most of these faults developed during delta progradation were syndepositional and also affect sediment dispersal. Fault growths usually coexist with slope instability towards the continental margin. Structural complexity in a local region reveals the density and fault style of such region. Simple structures such as crestal and flank are also present along individual faults. Hanging wall rollover anticlines are formed as a result of listric-fault geometry and differential loading of sediments of delta above ductile shales. Many complex structures that are cut by large number of faults with series of thrown include collapsed crest structures with domal shape

and extremely opposing fault dips at depth (Fig. 3). However; the main four structures reported by Doust and Omatsola (1990) are simple rollover structure with clay filled channel, structure with multiple growth faults, structure with antithetic fault, and collapsed crest structure (Fig. 3). The originated structural traps in the period of synsedimentary deformation of the Agbada formation, and stratigraphic traps developed selectively towards the flanks of delta usually describe the locations of the Niger Delta reservoirs. The primary seal rocks in the Niger Delta are the interbedded shale within the Agbada Formation (Doust and Omatsola, 1990; Owoyemi, 2004).

3. Materials and methods

The data used for this study comprises three–dimensional seismic data (SGY format), well header, well log data (LAS format), and check shot data. The data were collected from Nigerian Petroleum Development Company through the Department of Petroleum Resources, Ministry of Petroleum Resources, Lagos, Nigeria. Jemir field, an offshore (shallow water) field from Niger-Delta was used for the study while its total coverage was 113.2 km^2. Well logs comprise lithology, resistivity and porosity logs. Check shot data was used in the conversion of time values to depth, and for tying well log to seismic at the reservoir of interest.

A simplified procedure used to accomplish the desired task is presented in workflow diagram (Fig. 4). Well–to–seismic tie was done on individual field, reservoirs were identified and correlated across the wells along their respective horizon on seismic section. Structural traps were identified and their respective petrophysical parameters were estimated. In order to know the sealing potential of individual hydrocarbon bearing sand, horizon–fault intersection was done, volume of shale was determined, thickness of individual bed was estimated, and quality control involving throw analysis was done. Shale Gouge Ratio (SGR) and Hydrocarbon Column Height (HCH) (supportable and structure-supported HCH) were also determined to ensure the seal integrity of Jemir field. The seismic and well log data are integrated for the RCA and seal integrity study of tertiary Niger-Delta. Seismic data interpretation, well correlation, volume of shale analysis, and seal integrity study are often aimed at a qualitative and quantitative determination of the properties of a reservoir. These properties include the lithologic units, fluid content, porosity, thickness, level of shaliness and so on. It involves the use of seismic sections and well logs.

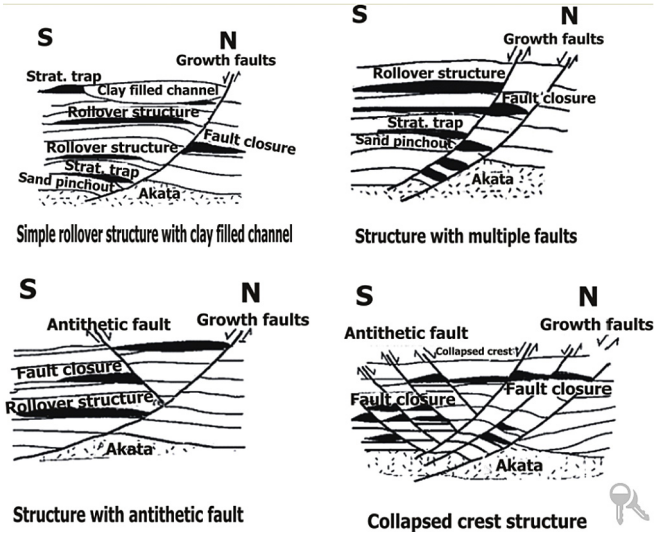

Fig. 3. Niger Delta oil field structures and associated trap types (Doust and Omatsola, 1990).

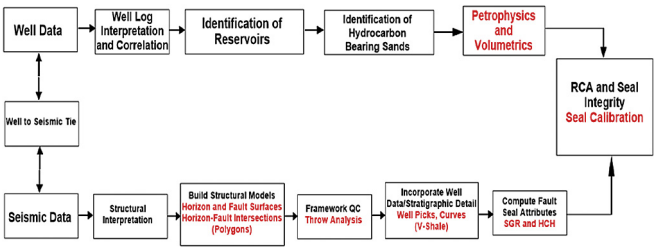

Fig. 4. Workflow diagram.

Mathematical models and automated techniques were employed for this research. The tools employed for this study were GeoGraphix version 5000.0.0.0 Licensed to Landmark Graphics Corporation (2008) and Trap Tester 7 by Badleys Geoscience Limited (2015). Seismic sections were interpreted in synergy with the existing borehole log(s) to create a more accurate image of the subsurface geology.

3.1. Interpretation procedures

For Petrophysics, well logging data can be interpreted qualitatively and quantitatively. Qualitative interpretation was carried out by means of visual observation of the characterization signature, shape, and patterns of the log of interest. Three points are the clue to qualitative log analysis:

i. type of lithology is indicated by the gamma ray log,
ii. hydrocarbon bearing region is known by resistivity logs, and
iii. neutron log in combination with density log is applied in order to delineate fluid contacts.

Qualitative interpretation is done using mathematical models to making geological inferences from the investigated reservoirs.

Volume of shale, porosity, water saturation, hydrocarbon saturation, bulk volume of water, net pay, original oil in place, and oil reserve were the steps to characterizing the reservoirs in the study area. Volume of shale was estimated based on Equation (1)

$$V_{Sh} = \frac{GR - GR_{clean}}{GR_{Sh} - GR_{clean}} \quad (1)$$

where: V_{Sh} = Clay volume or Shale volume, fraction; GR = Gamma ray reading from log, API;

GR_{Sh} = Gamma ray reading from shale, API;
GR_{Clean} = Gamma ray reading from sandstone formation, API

Average porosity was computed using Equation (2) while the effective porosity was estimated based on Equation (3).

$$\varnothing_A = \frac{\varnothing_D + \varnothing_N}{2} \quad (2)$$

where: $\varnothing_A$ = Average porosity; $\varnothing_D$ = Density derived porosity; $\varnothing_N$ = Neutron porosity (from log)

$$\varnothing_E = \varnothing_A \times (1 - V_{Sh}) \quad (3)$$

where: $\varnothing_E$ = Effective porosity; $\varnothing_A$ = Average porosity; V_{sh} = Volume of shale.

Hydrocarbon saturation was computed by directly subtracting the percentage water saturation from 100 (Equation (4)).

$$S_{hc} = 1 - S_w \tag{4}$$

where: S_{hc} = hydrocarbon saturation, %; S_w = water saturation.

Hydrocarbon pore volume was estimated based on Equation (5). It is given by the product of the porosity (Φ) and the hydrocarbon saturation ($1 - S_w$).

$$HCPV = \varnothing \times (1 - S_w) \tag{5}$$

Original oil in place can be estimated using Equation (6)

$$\text{OOIP} = 7758 \text{ X GRV X NTG X Porosity X (1-Water Saturation)} \tag{6}$$

where: 7758 = Conversion factor from acre-ft to barrel;

NTG = Net to Gross (i.e. percentage ratio of reservoir sand to the total rock volume);

$$\text{Gross Rock Volume (GRV) or Net Volume} = h \text{ X } A \tag{7}$$

where: h = Pay-thickness from Petrophysics; A = Area from 3-D Seismic interpretation

However, Stock Tank Original Oil in Place (STOOIP) was determined using Equation (8)

$$\text{STOOIP} = \text{OOIP} \div \text{Boi} \tag{8}$$

where: Boi = Oil Formation Volume Factor/Shrinkage Factor. Assumed Boi of 1.2 was used for the study.

Therefore Oil Reserve is given by Equation (9).

$$\text{Oil Reserve} = \text{STOOIP X Oil Recovery Factor } (RF_o) \tag{9}$$

For seal integrity, a Trap Tester project was created. The horizons, the fault segments, and the well data (i.e. well picks and Vshale curve) were imported into the Trap Tester project. The interpreted horizons and fault segments were further loaded into the volume editor for 3-D visualization and to build structural model. The fault attributes include: throw, stratigraphy, juxtaposition, shale gouge ratio (SGR) and hydrocarbon column height. All these were calculated in order to accomplish the seal integrity of the study area.

$$SGR = \frac{\sum(V - sh \times \Delta Z)}{t} \times 100\% \tag{10}$$

where: V-sh is the volume of shale, ΔZ is the thickness of the bed, and t is the throw.

The global SGR threshold for seal/leak fault is 20% (Yielding et al., 1997; Lawal, 2015).

Fault zone capillary entry pressure (FZP) was related to SGR based on Equation (11)

$$FZP(bar) = 10^{\left(\frac{SGR}{27-C}\right)} \tag{11}$$

where: C is the lifting correction (ms).

C is 0.5 for burial depths less than 3.0 km (9850 ft),
C is 0.25 for burial depths between 3.0 and 3.5 km (9850–11,500 ft), and
C is 0 for burial depth that is greater than 3.5 km (11,500 ft).

Column heights were calculated using fluid densities of 700 kg/m^3 for oil, 1035 kg/m^3 for water, and 0 was used for uplifting correction (C) since the deepest faults and horizons exceed 11, 500 ft (3.5 km).

Hydrocarbon buoyancy is calculated using Equation (12)

$$\Delta P = (\rho w - \rho h)gh \tag{12}$$

It is important to state that the pressure data were not given in the course of this study. However, Seal threshold pressure could be determined using the relationship of Berg (1975), Schowalter (1979), Watts (1987), and Ingram et al. (1997).

$$P_c = \frac{2\gamma \cos\theta}{r} \tag{13}$$

Combining and re-arranging Equations (12) and (13), h_{max} was estimated as:

$$h_{\max} = \frac{P_c}{g(\rho w - \rho h)} = \frac{2\gamma \cos\theta}{rg(\rho w - \rho h)} \tag{14}$$

where: P_c is the threshold pressure (Pascal (10^5 Pa = 1 bar)), γ is the surface tension (N/m),

θ is the wetting angles (°C), r is the pore throat radius (m),
H_{max} is the maximum hydrocarbon column height (m), ρ w is the pore water density (kg/m^3),
ρh is the hydrocarbon density (kg/m^3), and g is the acceleration due to gravity.

However, Lawal (2015) reported that Fault Zone Capillary Entry Pressure (FZP) is equivalent to threshold pressure (P_c) (such that FZP ≡ P_c) Also, threshold pressure was related to column height using Equation (15). The threshold pressure is converted to an equivalent hydrocarbon column height at every grid node on the fault surface. This was achieved via Trap Tester 7.

$$H_{\max} = \frac{FZP}{g(\rho w - \rho h)} \tag{15}$$

4. Results and discussions

4.1. Well log correlation

Fig. 5 shows a typical loaded well logs been correlated across individual horizon. The first track on each well is the gamma ray log that describes the lithology of the area by showing the gamma ray content; given that low gamma signifies a sandstone formation while high gamma signifies a shale formation. The second track on each well is the resistivity log. The resistivity log is also observed amongst the loaded well data. It helps to separate formations that contain water from formations that contain hydrocarbon.

It is important to determine how laterally distributed the identified reservoir formations are within the subsurface. In Fig. 5, the results of well correlation for Jemir field were achieved. Multiple reservoirs within the subsurface have been identified. Six reservoirs (reservoirs J Shallow, J1, J2, J3, J4 and J Deep) were mapped out on Jemir field. Five wells were drilled on Jemir field (Fig. 6) but one out these five wells is non-producing (precisely Jemir 5), only the gamma ray log exists on the well which made it to be exempted from the other wells. Therefore, four wells were eventually correlated on Jemir field (Fig. 5).

There is an upward and downward trend in reservoir variation across the correlated wells (Fig. 5) and not necessarily side by side in terms of depth, this can be as a result of the different faults acting in the subsurface of Jemir field. Some sandstone formations are of

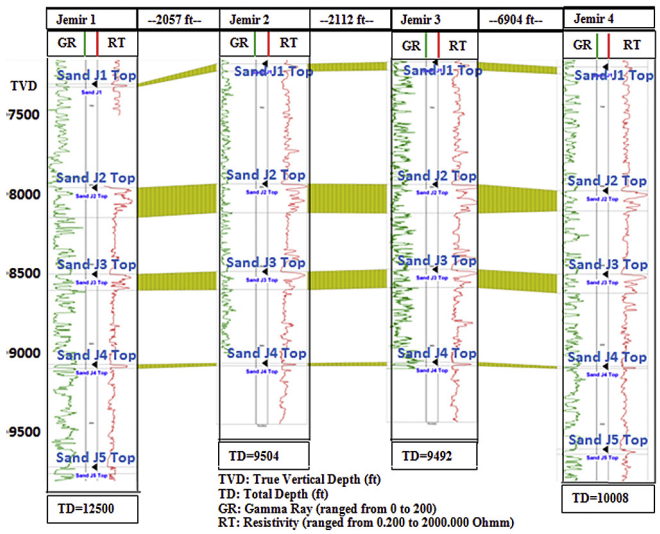

Fig. 5. Well log correlation of Jemir field.

little volume visually (reservoirs 1, 4, and 5) when compared to the sandstone formations of other reservoirs (reservoir 2 and reservoir 3). However, the shale/clay formations look almost similar across the wells. The prime use of shale is that it acts a seal to the reservoir. The shale above or below the reservoir can therefore be used to correlate the well log data.

4.2. Faults and horizons interpretation

The strike orientation of the fault is NW-SE while it dips towards south. Fault constitutes the structural trap in all the reservoirs. Fig. 6 showed the interpreted horizons, the fault(s) on the seismic sections, and the well(s) been tied to the seismic sections respectively.

Generally, the fault is resulted to a gap on a structure map between the formations in the hanging walls and the downthrown blocks. It gives rise to effective hydrocarbon traps closed by an anticlinal structure. The horizons were used to generate the seismic structural maps (i.e. the time and the depth structure maps).

4.3. Seismic structural maps

After seismic interpretation has been completed, fault heaves were calculated from the interpretation and the fault polygons

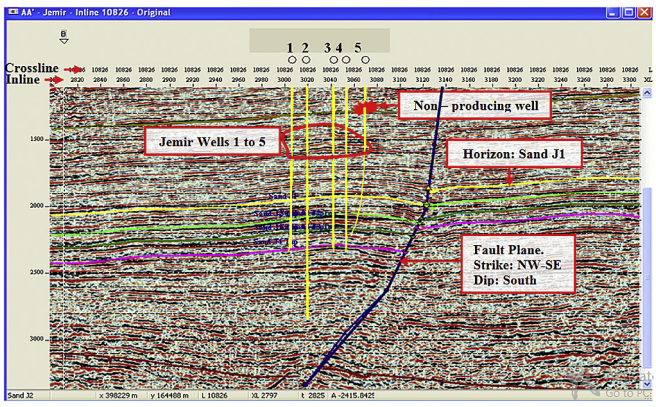

Fig. 6. Inline 10,876 of interpreted Horizons at Jemir Field.

were generated from the resulting heaves. The horizon time maps were gridded using the Seisvision gridding algorithm and the grids were exported to Geoatlas for the generation of the time structure map. These time structure maps with the check shots velocity data supplied were used to convert the seismic data from time to depth structures.

The time and depth structure maps were generated in order to estimate the hydrocarbon potential of the field. The time structure map was first generated and the depth structural map was later generated using the velocity model of each well. The time map shows the variation in time across the field while the depth map was used to analyze existing structures. Depth map was also used to locate and calculate the prospect areas.

Time structure maps were generated by joining lines of equal times on the base maps. It is a fault dependent structure. Six (6) time structure maps were generated at Jemir field (Fig. 7a to f). The time signatures on Fig. 7a ranged from 1170 ms to 1480 ms. The bold contours have interval of 50 ms while the interval of regular contours were 10 ms respectively. Only one fault (the major fault) appeared on the map with the time signatures ascending from NE-SW direction. The closure on the map was independent of fault.

The time signatures on Fig. 7b ranged from 1770 ms to 2130 ms. The bold contour also have the interval of 50 ms while the regular contours have interval of 10 ms. Some of the closures on the map were fault dependent while others were relatively close to the major fault on the map. The time signatures also ascended from NE-SW direction.

Fig. 7c has relative structure of Fig. 7b (time map of J1). The time signatures ranged from 1860 ms to 2280 ms. The bold contour and the regular contour interval were the same with the previous maps.

A major fault passes through horizon J3 on Jemir field in NW-SE orientation (Fig. 7d). Some of the closures were fault dependent while others were relatively close to the fault. The time ranged from 1940 ms to 2370 ms. The orientation of the time signatures was also in the NE-SW direction.

Fig. 7e closures were fault dependent. A minor fault was noticed towards the northern side of the field with the major fault trending in NW-SE direction. The time signatures ranged from 2020 ms to 2490 ms. The contour intervals and the diverging nature of the time map were the same with the previous maps.

Fig. 7f showed fault dependent and independent of fault closures. The time ranged from 3130 ms to 3450 ms. Sand J Deep, however has series of closures in different directions which made its structures to be different from other time structure maps.

To generate the depth map, velocity model is developed from the check shot data. The map depicts the depth to the top of the prospective reservoirs at different locations. It is observed that close contours could represent traps for hydrocarbon content as delineated by the petroleum system of the Niger-Delta region. Most of the traps of the Niger-Delta are fault dependent, hence, more interest lie on areas where there is a contour closing on a fault and characterized by a peak in resistivity on the resistivity log. Seal integrity study would further be carried out to confirm if the traps are sealing or leaking.

Six (6) depth maps were generated at Jemir field (Fig. 8a to f). The structure on the depth map of J-Shallow (Fig. 8a) was fault independent. For this reason, further analysis on this horizon is unnecessary. The second horizon; J1 depth map (Fig. 8b) is fault dependent with anticlinal structure. The discovery zone bounded out by contour line of 7300 ft. The direction of hydrocarbon migration on the depth map ranged from eastern side of the field to the central part of the field. This suggests the reason why the four (4) producing wells on Jemir field were drilled at the central part of the field (bounded by contour line of 7250 ft). The contour interval of 50 ft was used for all Jemir depth maps. Horizon J1 showed

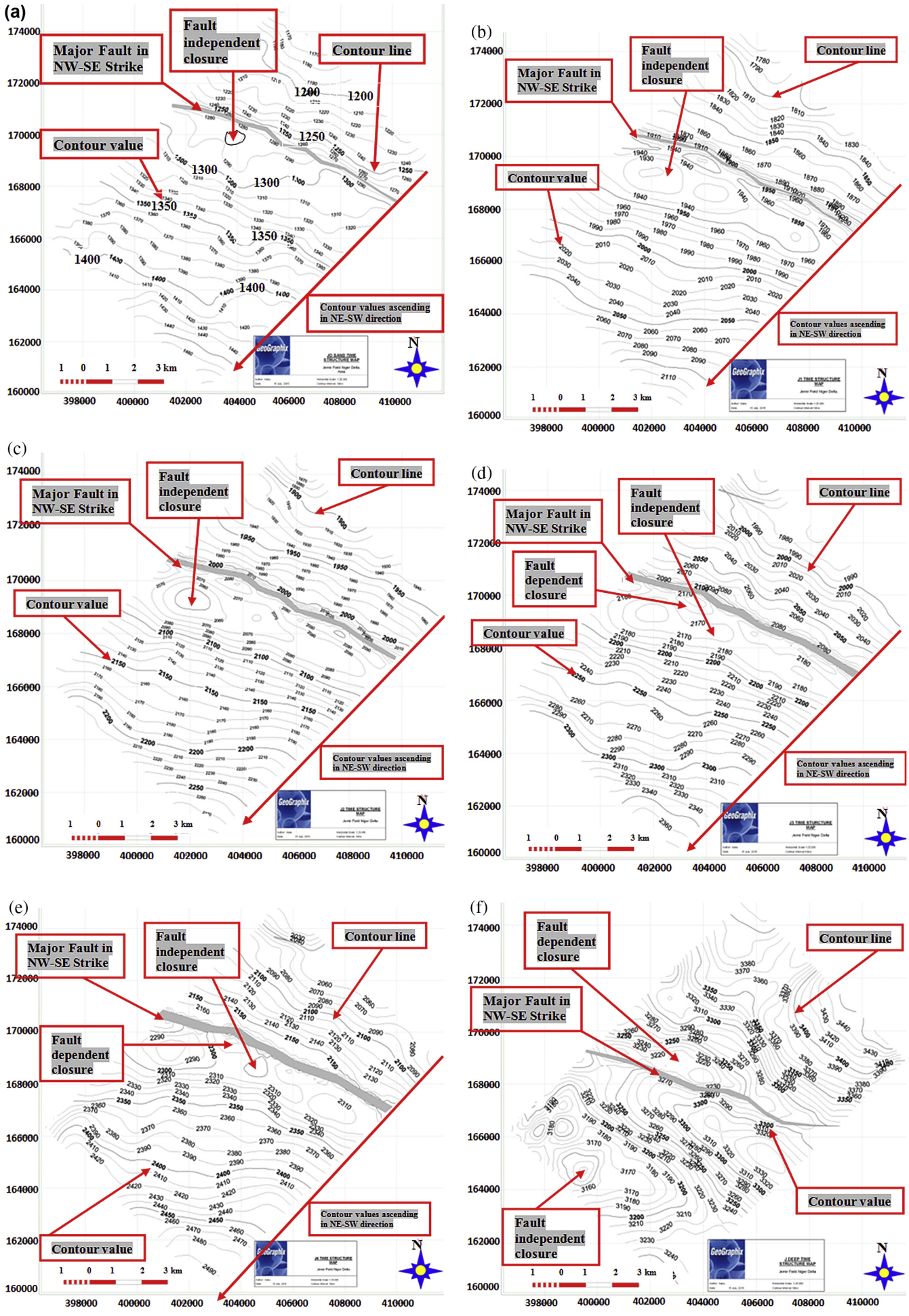

Fig. 7. a: Time Structure Map of Sand J Shallow on Jemir Field. b: Time Structure Map of Sand J1 on Jemir Field. c: Time Structure Map of Sand J2 on Jemir Field. d: Time Structure Map of Sand J3 on Jemir Field. e: Time Structure Map of Sand J4 on Jemir Field. f: Time Structure Map of Sand J Deep on Jemir Field.

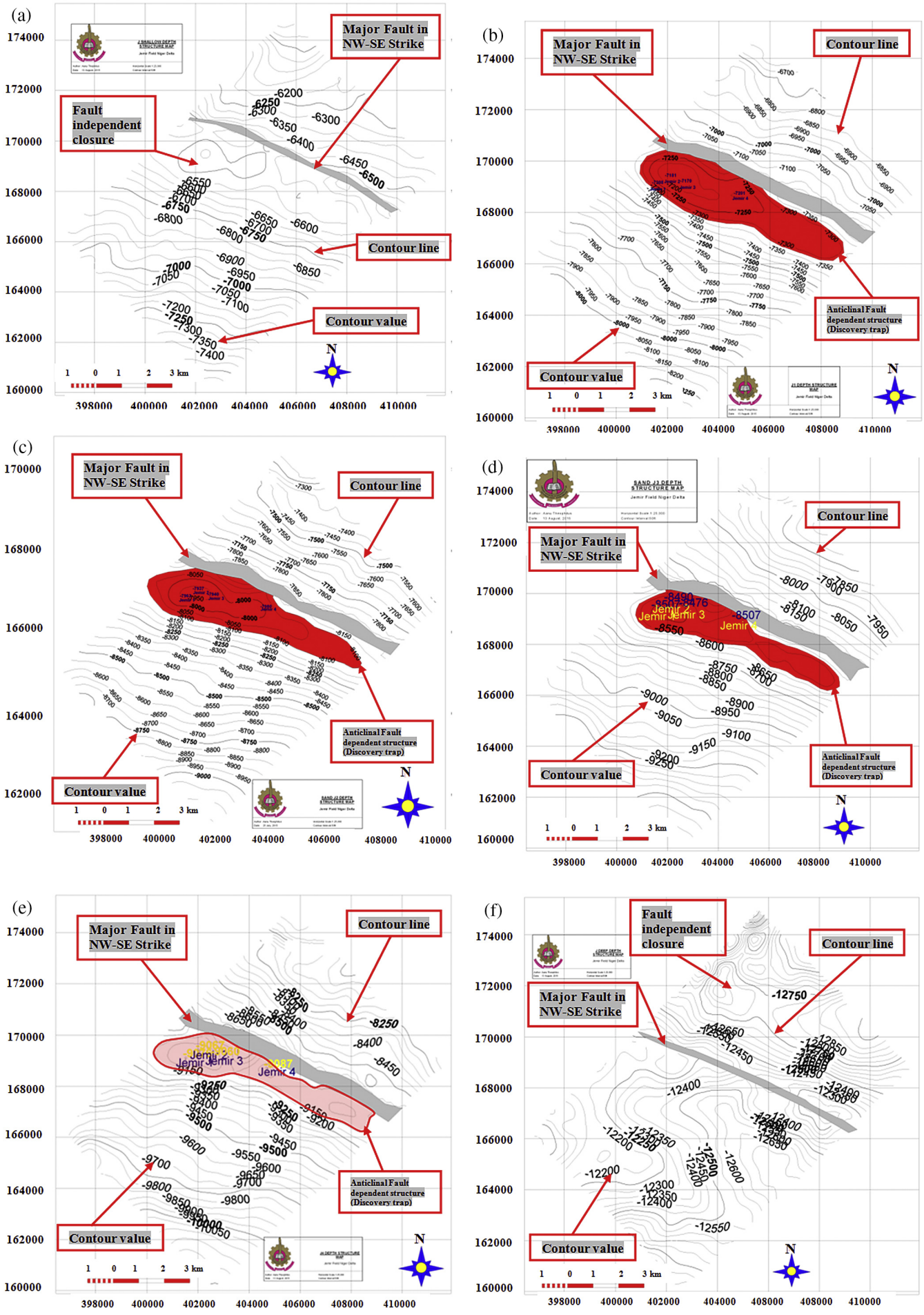

Fig. 8. a: Depth Structure Map of Sand J-Shallow on Jemir Field. b: Depth Structure Map of Sand J1 on Jemir Field. c: Depth Structure Map of Sand J2 on Jemir Field. d: Depth Structure Map of Sand J3 on Jemir Field. e: Depth Structure Map of Sand J4 on Jemir Field. f: Depth Structure Map of Sand J-Deep on Jemir Field.

Table 1a
Petrophysical parameters of Jemir field.

Wells	Top MD (ft)	Base MD (ft)	Top TVDSS (ft)	Base TVDSS (ft)	Gross Interval (ft)	Net Reservoir (ft)	Net Pay (ft)	NTG	Phi A	Sw
Sand J1										
Jemir 1	7, 366.39	7, 384.41	−7, 308.07	−7, 326.08	18.01	9.00	5.00	0.50	0.22	0.40
Jemir 2	7, 229.83	7, 277.22	−7, 180.64	−7, 227.89	47.26	46.23	14.00	0.98	0.29	0.51
Jemir 3	7, 222.97	7, 273.67	−7, 170.15	−7, 220.78	50.63	42.00	17.00	0.83	0.25	0.44
Jemir 4	7, 251.41	7, 295.41	−7, 200.61	−7, 244.49	43.88	40.96	–	0.93	–	–
Sand J2										
Jemir 1	8, 020.23	8, 208.19	−7, 961.72	−8, 149.66	187.94	129.50	70.50	0.69	0.22	0.34
Jemir 2	7, 988.13	8, 170.74	−7, 936.69	−8, 118.95	182.26	177.47	100.50	0.97	0.26	0.40
Jemir 3	7, 993.48	8, 175.90	−7, 939.71	−8, 121.98	182.26	–	–	–	–	–
Jemir 4	8, 032.95	8, 161.49	−7, 980.30	−8, 108.56	128.27	82.55	54.50	0.64	0.24	0.34
Sand J3										
Jemir 1	8, 565.20	8, 667.39	−8, 506.55	−8, 608.69	102.15	48.00	38.50	0.47	0.21	0.40
Jemir 2	8, 542.38	8, 657.21	−8, 490.22	−8, 604.98	114.76	105.94	33.00	0.92	0.24	0.31
Jemir 3	8, 530.50	8, 645.30	−8, 476.38	−8, 591.14	114.76	–	–	–	–	–
Jemir 4	8, 560.29	8, 678.54	−8, 506.85	−8, 624.98	118.14	83.46	38.46	0.71	0.23	0.36
Sand J4										
Jemir 1	9, 134.69	9, 160.31	−9, 075.88	−9, 095.00	19.12	14.50	12.50	0.76	0.20	0.47
Jemir 2	9, 119.77	9, 136.64	−9, 067.39	−9, 084.26	16.87	–	–	–	–	–
Jemir 3	9, 114.57	9, 138.20	−9, 060.30	−9, 083.93	23.63	–	–	–	–	–
Jemir 4	9, 141.38	9, 154.90	−9, 087.40	−9, 100.90	13.51	–	–	–	–	–

Hint: GRV is the Gross Rock Volume, NTG is the Net to Gross, Sw is the water saturation, OOIP is the Original Oil in Place, TVDSS is the Total Vertical Depth Subsea, and Phi A is the same as Porosity, and STOOIP is the Stock Tank Original Oil in Place.

Table 1b
Average volumetric analysis of Sand J1 to Sand J4 in Jemir field.

Sand	Area (Acres)	GRV (Acreft)	NTG	Porosity	Sw	OOIP (bbl)	STOOIP (bbl)
J1	3, 436	239, 055	0.81	0.25	0.45	208, 105, 629	173, 421, 357
J2	2, 924	199, 222	0.77	0.24	0.36	184, 464, 411	153, 720, 343
J3	3, 489	233, 955	0.70	0.23	0.35	185, 319, 525	154, 432, 938
J4	558	10, 517	0.76	0.20	0.47	6, 543, 109	5, 452, 591

increasing contour trend from NE-SW direction which ranged from 6650 ft to 8300 ft. No new prospect was identified since only one closure exists on J1 depth map.

However, J2 to J4 depth maps (Fig. 8c to e) have almost the same structure as that of J1 depth map (Fig. 8b). The fault dependent closure of J2 (Fig. 8c) is bounded by contour line 8100 ft. The contour ranged from 7200 ft to 10,050 ft. The fault dependent closure of J3 (Fig. 8d) was bounded by contour line 8550 ft. The contour ranged from 7650 ft to 9600 ft. J4 depth map (Fig. 8e) is also a fault dependent closure bounded by contour line 9150 ft. The contour ranged from 8000 ft to 10,200 ft. However, the depth maps J-Shallow, J1, J2, J3 and J4 all showed increasing contour trend from NE-SW direction. Only the J-Deep depth map (Fig. 8f) has different orientation. No reasonable prospect could be identified on the map. Therefore, further analysis on J-Deep depth map was unnecessary.

4.4. Petrophysical analyses

The results of the interpreted well logs revealed that the hydrocarbon interval in the study area occurred between the depths 7266.39 ft (2201.9 m) to 9154.90 ft (2774.2 m). Well correlations are crucial in Petrophysics because it is the well correlation that helps interpreter to identify individual reservoirs (sand bodies) that are present in the well by observing intervals where the gamma ray log reads relatively low values (i.e. deflection to the left). The reservoirs varied in thicknesses, some were hydrocarbon bearing while some were water bearing. The fluid content and contact (oil water contact) was determined using the resistivity log since hydrocarbon is more resistive than water.

Jemir field is an oil field. Based on the analysis, Tables 1a and 1b are the petrophysical parameters and volumetric estimation of Jemir field respectively. Porosity estimation of Jemir field ranged from 0.20 (sand J4, Jemir 1) to 0.29 (sand J1, Jemir 2) (Table 1a). The net to gross ranged from 0.50 (sand J1, Jemir 1) to 0.98 (sand J1, Jemir 2). These results showed that reasonable hydrocarbons were trapped on Jemir field. Table 1b is the average volumetric estimation results of the sands in Jemir field since there was no new prospect on the field. Sand J1 stock tank original oil in place (STOOIP) was estimated to be 173, 421, 357 bbl, sand J2 was estimated to be 153, 720, 343 bbl, sand J3 was estimated to be 154, 432, 938 bbl and sand J4 was estimated to be 5, 452, 591 bbl respectively. Jemir 4 of sand J1 was non-hydrocarbon bearing sand, Jemir 3 of sand J2 and Jemir 3 of sand J3 were also non-

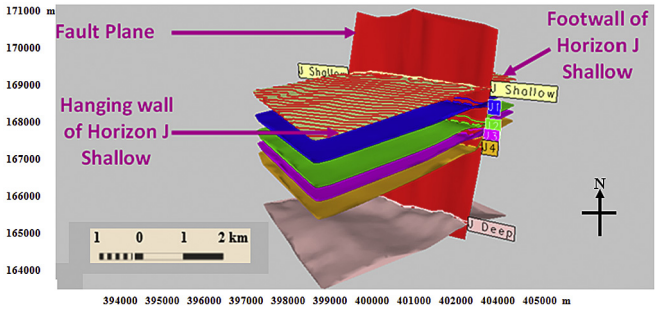

Fig. 9. Structural model of Jemir field.

hydrocarbon bearing sand. However, only Jemir 1 was hydrocarbon bearing on sand J4. This could have been as a result of poor sealing which has caused the hydrocarbon to migrate out of the trap.

4.5. Structural interpretation

Horizon and fault interpretations were used to build the structural model. A framework model is a three-dimensionally consistent set of intersecting fault and horizon surfaces. Data used to build the structural model are horizons and fault interpretations. The raw fault segments were automatically modeled into a 3-D fault surface. Spikes or jumps in the fault surface refer to irregularities in the interpretation of the fault segments. Branch line (i.e. line of intersection between two faults) was created to generated a relationship between the major (master) and minor (splay) faults in order to link the two together (fault network).

Synchronization of fault surfaces and the horizons in the volume editor of Trap Tester 7 was used to model the intersection between the horizon raw data and the fault surfaces. The structural model of Jemir field was presented on Fig. 9.

4.6. Fault attributes calculations and seal analyses

Fault attributes involve calculations of vertical displacement between two faults and generation of modeled maps. The fault attributes include: volume of shale (V-shale), throw, stratigraphy, reservoir-juxtaposition, shale gouge ratio (SGR), and hydrocarbon column height. However, SGR estimation (Equation (10)) and its algorithm are the essential in the prediction of seal integrity of a fault plane.

4.6.1. Volume of shale

Volume of shale (V-shale) models (Fig. 10a–d) are derived product, typically from gamma ray log which is not necessarily the same as the actual volumetric clay content of the rock. The main assumption is that sand and shale material are incorporated into the fault, fault gouge in the same proportions (ratio) as they occur in the wall rocks of the slipped interval. Prediction of whether or not all or part of a fault plane is sealing in terms of juxtaposition and SGR requires an accurate determination of shale volume from log data. The V-Shale ranged from 0 to 1 because it is in fraction and has no unit. High V-Shale rating (≥ 0.4) indicates sealing while low V-Shale rating indicates leaking zone (Rider, 2000).

The V-Shale log strip of Jemir field is shown on Fig. 10a and b respectively. The log has 57-shale markers. The depth of markers ranged from 6000 ft to 12,200 ft. 3-D map generated from footwall plane of Jemir field (Fig. 10c) showed that the top and the bottom of the plane are leaking (characterized with low V-Shale). However, high V-Shale occurred few feet away from the base of the fault through the middle. The same structure of footwall is also experienced on the hanging wall (Fig. 10d) of Jemir field. If horizons are

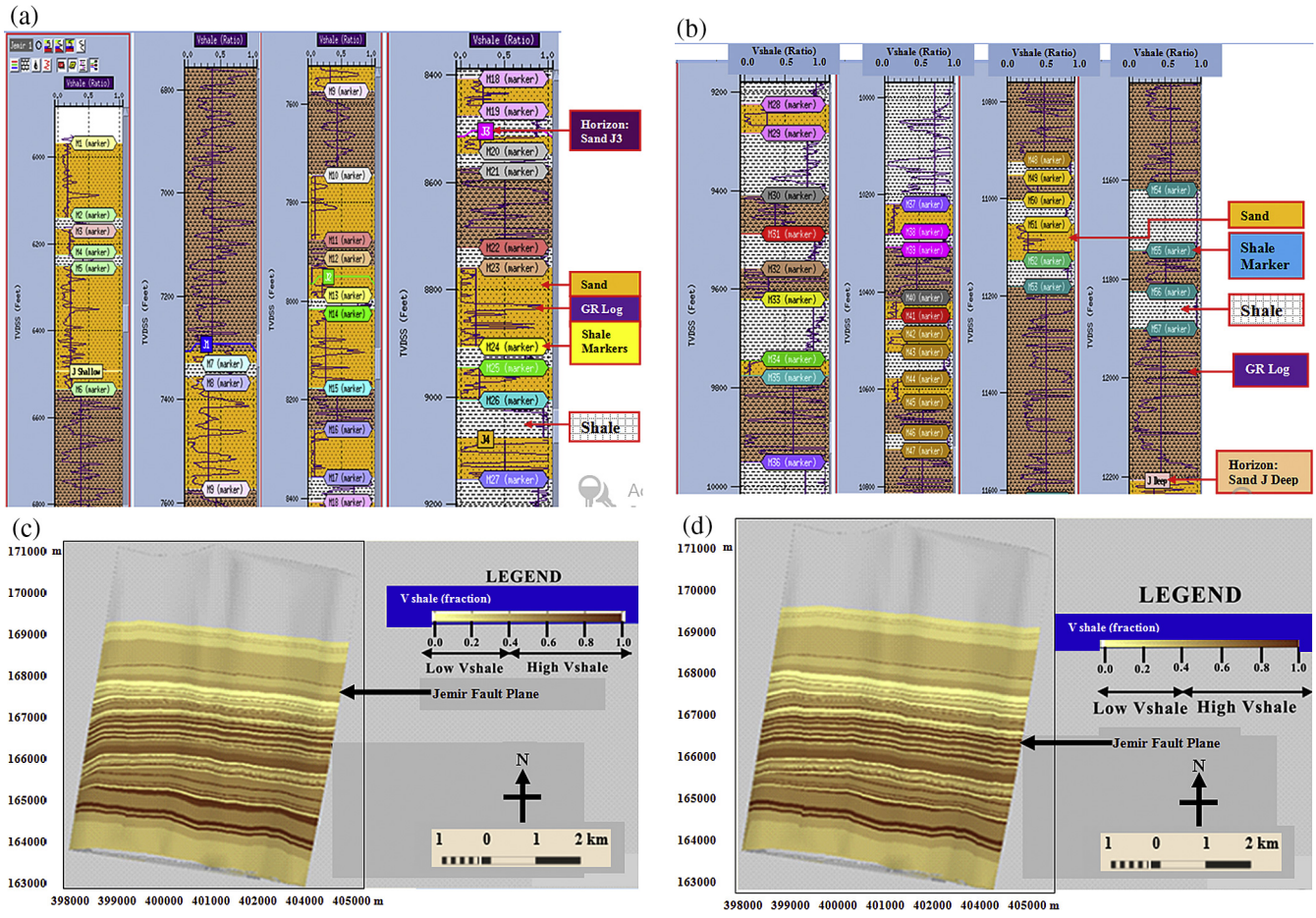

Fig. 10. a: V-shale log Strip of Jemir Field (from depth 6000 ft–9200 ft). b: V-shale log Strip of Jemir Field (from depth 9200 ft–12,200 ft). c: 3-D of Vshale along footwall of Jemir field. d: 3-D of Vshale along hanging wall of Jemir field.

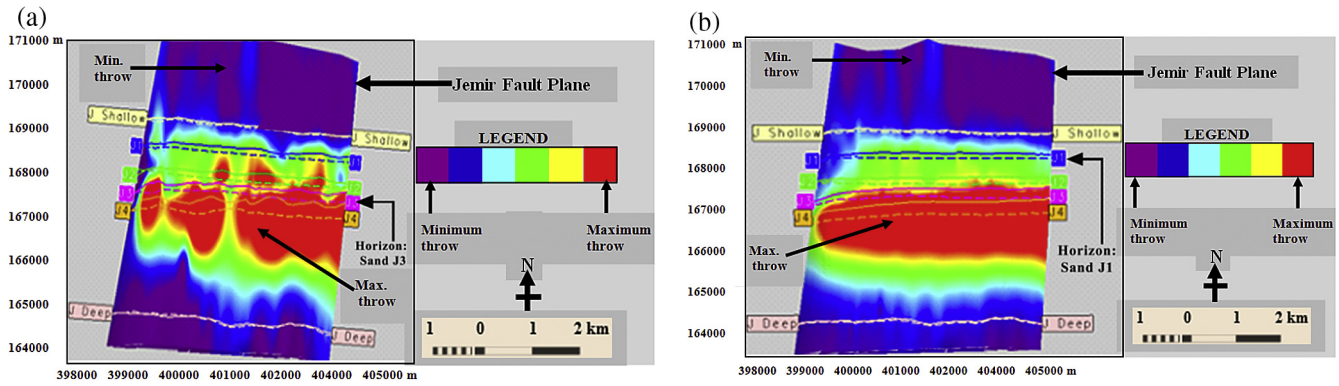

Fig. 11. a: Unedited throw distribution. b: Edited throw distribution.

present along the zone with low V-Shale, there is tendency for the plane to be leaking.

4.6.2. Throw distribution

The quality of the fault-horizon intersection lines (fault-polygons) were assessed and edited. The unedited horizon polygons were used to generate unedited throw. The danger of using unedited throw for interpretation is that abrupt irregularities (noise) in the polygons geometry may reflect anomalies in the interpretation. After the horizon polygons have been edited, the true natures of the throw distribution on the investigated Jemir field was revealed. Unedited throw of Jemir field was presented on Fig. 11a while the edited throw was presented on Fig. 11b.

On an ideal situation, isolated normal fault, fault displacement and fault polygons vary in systematic manner across a fault surface. The basic pattern can be modified by fault interaction and growth. Therefore, analysis of throw distribution on a fault provides an effective method for quality checking of the intersection model.

The hanging wall is the major contributor to the accumulation of hydrocarbons since it is the moving part of the fault. The centre of the throw is always its maximum displacement (characterized by red colour). Jemir field throw represents normal throw distribution. The red colour at the middle of the throw showed maximum displacement, followed by the yellow, green light blue, blue and purple colour (towards both tips). The purple colour indicates minimum throw distribution.

4.6.3. Stratigraphy

Stratigraphy means variation in lithology with depth (i.e. the intercalation of sand and shale). The stratigraphy of Jemir field along the footwall was presented on Fig. 12a while the stratigraphy along the hanging wall was presented on Fig. 12b. Sandstone started the first lithology with some shale which intercalated the lithology. Shaly sandstone also covered some lithologic formation both at the footwall and hanging wall of the major fault. The three stratigraphy identified necessitate the seal analysis of the reservoirs.

4.6.4. Reservoir juxtaposition

Fault sealing properties are controlled by the juxtaposition of reservoir against sealing lithologies, deformation during fault displacement and subsequent evolution and current state of stress of the fault has proximity to failure. With the stress state of fault relates to the in situ stress state of fault and the critical stress state at which a fault may leak (Maunde et al., 2013). Juxtaposition relates to detailed mapping of an area to identify reservoir-reservoir juxtaposition and possibilities of a non-permeable lithology forming a side seal to reservoirs across a fault plane. Although in reservoir-reservoir juxtaposition, the possibility of seal still exists if the fault zones have capillary pressure higher than reservoirs on either side of it.

Reservoir juxtaposition represents a first order fault-seal analysis. Horizons picked during seismic interpretations are often too widely spaced for detailed seal integrity. Additional stratigraphic information, mainly derived from well data, must be incorporated into the analysis.

Isochore surfaces within the entire 3D model based on well information were generated. The tops represent sands picked in the well equivalent to the seismic horizons, while the bases represent the shales.

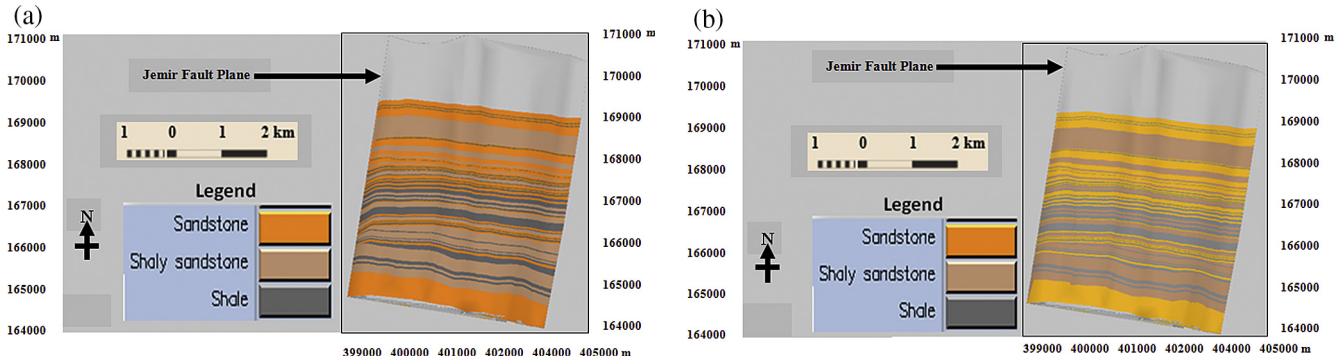

Fig. 12. a: Stratigraphy of Footwall on major Fault of the Jemir Field. b: Stratigraphy of Hanging Wall on major Fault of the Jemir Field.

The gray colour are either shale-on-shale, shale-on-sand, or sand-on-shale juxtaposition (i.e. shale in the footwall which juxtaposed shale in the hanging wall, shale in the footwall which juxtaposed sand in the hanging wall, or sand in the footwall which juxtaposed shale in the hanging wall). Other colours are sand-on-sand juxtaposition.

The shale-on-shale, shale-on-sand, or sand-on-shale juxtaposition has high sealing potential while sand-on-sand juxtaposition is likely to be leaking. However, sand-on-sand juxtaposition was done on sand-on-sand zone along the fault plane of Jemir field in order to detect the leaking horizon(s) from the hydrocarbon bearing horizons.

Fig. 13 showed that the area marked with black circle has the ability to leak because it is the only region within the hydrocarbon bearing horizons that showed least sand-on-sand juxtaposition (green colour) along the fault plane. However, this cannot be relied on as the major determinant of fault sealing and leaking are the estimation of shale gouge ratio and the estimation of hydrocarbon column height (Sahoo et al., 2010; Maunde et al., 2013).

4.6.5. Shale gouge ratio (SGR)

Shale gouge ratio (SGR) was computed along the fault plane using the thickness of the bed, average V-Shale from the hanging wall and the footwall as well as the throw distribution across the fault plane (Yielding et al., 1997; Yielding, 2002). The SGR was calculated based on Equation (10). The SGR is a prediction of the amount of clay or shale material in the fault zone. A high SGR equates to a high proportion of clay or shale material in the fault plane. The higher the SGR, the greater the across-fault seal potential. Based on Sahoo et al. (2010), the SGR were grouped into four zones: leaking fault (green colour), poor sealing (yellow colour), moderate sealing (orange colour) and sealing fault (red colour). However, low SGR was depicted by green colour while high SGR was depicted by red colour.

SGR was calculated and its 3D model was generated. Sand-on-sand juxtaposition was further employed in other to see if the hydrocarbon bearing horizons are sealing or leaking. Fault commonly contains a sheared mélange where the fault offset is greater than the bed thickness. So SGR is mainly studied in the interval where fault throw is greater than the bed thickness. For simpler calculation purpose fault zones are taken as single fault. Taking reference from Yielding et al. (1997), a generalized classification of faults is made based on SGR values. SGR < 0.2 (<20%) are typically associated with cataclastic fault gouge and sealing of the fault is considered as unlikely. A cataclastic rock is a type of metamorphic rock that has been wholly or partly formed by the progressive fracturing and comminution of existing rock, a process known as

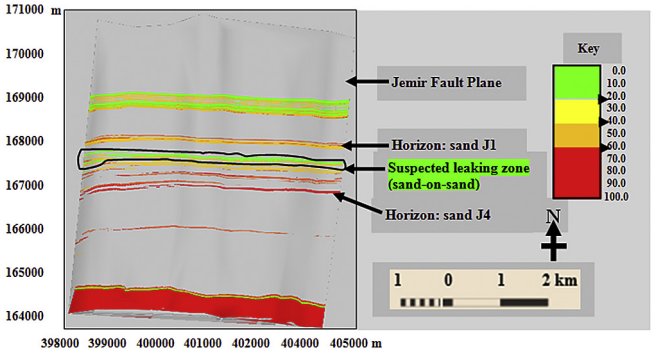

Fig. 13. Sand-on-Sand juxtaposition of Jemir field.

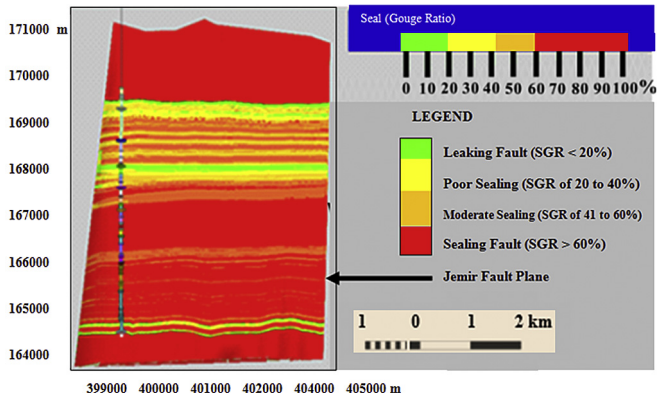

Fig. 14. SGR of Jemir field.

cataclasis, and is mainly associated with fault zones. Comminution is the reduction of solid materials from one average particle size to a smaller average particle size during faulting. Yielding et al. (1997) reported that Shale Gouge Ratio < 20% correlates with leaking fault while SGR > 20% correlates with greater fault seal potential. However, Sahoo et al. (2010) further categorized shale gouge ratio > 20% into three (3) groups. SGR from 20 to 40% (0.2–0.4 v/v) is associated with phyllosilicate framework and some clay smear fault rocks. Here fault is taken as poor seal and will be retarding to fluid flow. For SGR from 40 to 60% (0.4–0.6 v/v), fault is considered to be moderately sealed. It will be associated mainly with clay smears. For SGR > 60% (>0.6 v/v), fault is taken as a likely sealed fault.

In this study, SGR less than 20% is associated with leaking fault, SGR of 20–40% is associated with poor sealing, SGR of 40–60% is associated with moderate sealing, while SGR greater than 60% is associated with sealed fault. Fig. 14 showed the top and bottom of the fault plane of Jemir field to be sealing. Some leaking, poor sealing and moderate sealing zones were shown towards the upper part of the fault plane. Analysis of this region is paramount because it constitutes where the hydrocarbon bearing horizons are located. However, Fig. 15 showed horizon J1 to horizon J4 been displayed on SGR of Jemir field. Horizon J-Shallow and J-Deep were exempted because the petrophysical analysis showed the two horizons were non-hydrocarbon bearing sands. Horizon J1 was located a bit higher than the leaking zone (SGR < 20%) along the fault plane. This has enabled the hydrocarbon to be trapped in reservoir J1 but the horizon was located on a poor sealing zone which suggests that over some period of time, hydrocarbon would migrate from this trap due to the nature of its sealing. Horizon J2 to horizon J4 showed that the fault plane supporting these traps belong to moderately sealed fault plane. Since perfect sealing is not guaranteed in moderate seal, leakage is also associated with this type of seal.

Gray colour on Fig. 15 denotes either shale-on-shale, shale-on-sand, or sand-on-shale juxtaposition while other colours denote sand-on-sand juxtaposition. The reason why zones with sand-on-sand juxtaposition that are associated with low SGR along the plane were non-hydrocarbon bearing sands from the logs is that the hydrocarbons have migrated from the trap due to communication between the hanging wall and the footwall. Horizons J1 is supported with poor sealing while horizon J2 to horizon J4 showed moderate sealing across the fault plane (i.e. from the hanging wall through the plane to the footwall). This outcome justified the reason why the four horizons are still hydrocarbon bearing sands.

However, the SGR inferences would be validated if the results of supportable hydrocarbon column height are almost the same with

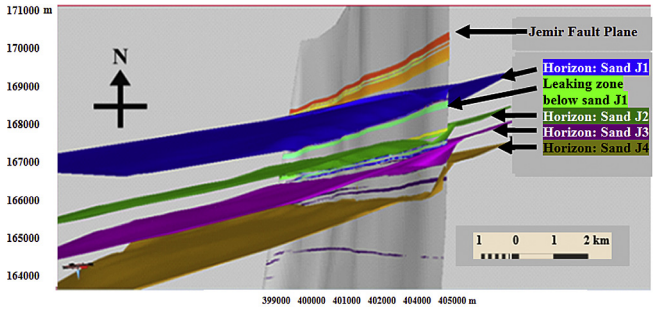

Fig. 15. SGR and some Horizons of Jemir Field.

that of structure-supported hydrocarbon column height on each horizon. If otherwise, gradual leakage of hydrocarbon from trap is possible.

4.6.6. Hydrocarbon column height (HCH) estimation

Estimation of fault-zone composition using the shale gouge ratio (SGR) can be empirically calibrated with pressure data to define depth-dependent seal-failure envelopes. The relationships between SGR, fault zone capillary entry pressure (FZP), and hydrocarbon column height (HCH) have been presented from Equations (10) to (15).

Estimation of hydrocarbon column heights using seal attributes depends on the geologic input to model, in particular, pressure data, volumetric shale fraction, and the precision of the three dimensional mapping of reservoir geometry in the vicinity of the fault. Though pressure data were not given, the threshold pressure has been calculated based on Equation (15). In a hydrocarbon-water system, leakage of hydrocarbons through a water-wet fault zone is by capillary action. Leakage of hydrocarbons through the fault zone takes place when the difference in pressure between the water and hydrocarbon phases (buoyancy pressure) exceeds the pressure required for hydrocarbons to enter and pass through the largest interconnected pore throat in the seal (displacement or capillary entry pressure). In this context, the pore-throat size in a fault zone controls capillary entry pressure. In general, the smaller the pore-throat size, the higher the capillary entry pressure required for the seal to fail, and the greater the hydrocarbon column that can potentially be supported.

Maximum height of the hydrocarbon column supported by given SGR value and the structure-supported hydrocarbon column height were presented on Table 2. Though the SGR of the investigated fields mostly belong to poor sealing category (SGR from 20 to 40%), the wide difference between the supportable HCH and the structure-supported HCH confirms gradual leakage across the fault planes of Jemir field. Sand J2 of Jemir field has minimum SGR of 13.6%, this indicates that some of hydrocarbons in this horizon have been migrated out of the trap. However, it might have been that hydrocarbons in sand J-Shallow and sand J-Deep of Jemir field have migrated out of these horizons due to low SGR. This confirmed the reason why they are non-hydrocarbon bearing horizons. Due to these analyses, it is revealed that migration of hydrocarbon is possible from traps in as much as the shale gouge ratio of hydrocarbon bearing sands ranged from poor to moderate sealing category. However, SGR <20% is associated with leaking fault and could not even support hydrocarbons in fault dependent structures.

5. Conclusions

An attempt has been made on the reservoir characterization and seal integrity of Jemir field in Niger Delta, Nigeria. The study has shown the importance of evaluating reservoir's properties and its seal integrity, as a method of reducing the risk of drilling dry well and reducing the uncertainty of overestimation of hydrocarbons in a field without considering if the faults supporting the traps are sealing or leaking. The integrity of the fault-dependent closures was analyzed and the area of leakage and sealing parts of the fault were identified. Migration of hydrocarbon from trap is possible when fault leaks. Faults in the subsurface generally have compartmentalization and sealing properties. These properties are usually delineated by the amount of shale on the fault plane, performance of flow monitoring and performance in reservoirs and identifying variations in oil contacts across a fault plane. It was inferred that poor sealing constitute most of the hydrocarbon bearing sands in Jemir field.

From the petrophysical parameters of Jemir field showed that its porosity ranged from 0.20 to 0.29. Porosity indicates how much fluid a rock can hold. This affirms that the porosity of Jemir field is good enough for hydrocarbon production since Horsfall et al. (2013) reported that reservoirs have porosity values within the range of 5–30%. However, the oil reserve estimated showed a good pay of 5.5–173.4 Mbbl.

The SGR estimated ranged from leaking fault (SGR < 20%) to sealing fault (SGR > 60%). It was revealed that none of the horizons belong to the leaking zone (green colour) but most of the hydrocarbon bearing horizons on the fields were supported by poor sealing fault plane (SGR from 20% to 40%). The implication is that with time, migration of hydrocarbons from traps through the fault planes is possible because of improper sealing of these faults.

Estimation of supportable HCH of Jemir field ranged from 98.3 to 446.2 m while its structure supported HCH ranged from 12.1 to 101.7 m. It was observed that in all, the supportable HCH was not the same as the structure-supported HCH. This variation is concluded to either be as a result of leaking faults supporting the traps or the traps being hindered by fault against appropriate charge. However, quick exploitation of hydrocarbons from these reservoirs is recommended before it is too late.

Table 2
Supportable and structure-supported hydrocarbon column heights Jemir field.

Interval	Minimum SGR (%)	Supportable Hydrocarbon Column Height (ft)	Structure-Supported Hydrocarbon Column Height (ft)	Difference between Supportable HCH and Structure-Supported HCH (ft)
Sand J-Shallow	–	–	–	–
Sand J1	36.7	516.9	143.2	373.7
Sand J2	13.6	783.7	41.6	742.1
Sand J3	40.0	1472.5	335.6	1136.9
Sand J4	45.8	324.5	40.0	284.5
Sand J-Deep	–	–	–	–

Acknowledgement

The authors are grateful to the assistance rendered by the Department of Petroleum Resources, Ministry of Petroleum Resources, Nigeria and Nigerian Petroleum Development Company for providing the data used for this study. We are also grateful to Badley Geoscience Limited and Landmark Graphics Corporation for creating the automated links used for the study. The critical and thoughtful reviews of the anonymous reviewers of J. of African Earth Sciences are highly appreciated. Finally, Dr. T.A. Adagunodo specially acknowledges the contributions of the Board of Postgraduate School in LAUTECH led by Prof. L.A. Sunmonu, Prof. Joseph Adeniyi Olowofela (Hon. Commissioner for Education, Science and Technology in Oyo State, Nigeria), Prof. Frank T. Ebijuwa, Prof. O.O. Fawole, Prof. A.A. Odunsi, Prof. E.T. Ayodele, Prof. A.O. Awodugba, Prof. A.A. Raheem, Prof. A.W. Ogunsola, Dr. Y.K. Sanusi, Dr. O.G. Bayowa and Mr. Yusuf Olanrewaju Odusanwo towards the success of this research.

References

Amadi, A.N., Olasehinde, P.I., Yisa, J., Okosun, E.A., Nwankwoala, H.O., 2012. Geostatistical assessment of groundwater quality from coastal aquifers of eastern Niger Delta, Nigeria. Geosciences 2 (3), 51–59.

Ameloko, A.A., Omali, A.O., 2013. Reservoir characterization and structural interpretation of seismic profile: a case study of Z-field, Niger Delta, Nigeria. Pet. Coal 55 (1), 37–43.

Badleys Geoscience Limited, 2015. Reference manual. Trap Tester 7. P 4.1–4.12.

Berg, R.R., 1975. Capillary pressures in stratigraphic traps. Am. Assoc. Pet. Geol. Bull. 59, 939–956.

Doust, H., Omatsola, E., 1989. Niger Delta. AAPG Mem. 48, 201–238.

Doust, H., Omatsola, E., 1990. Niger Delta. In: Edwards, J.D., Santogrossi, P.A. (Eds.), Divergent/passive Margin Basins, AAPG Memoir 48, Tulsa. American Association of Petroleum Geologists, pp. 239–248.

Eshimokhai, S., Akhirevbulu, O.E., 2012. Reservoir characterization using seismic and well logs data (a case study of Niger Delta). Ethiop. J. Environ. Stud. Manag. 5 (Suppl. 2), 597–603 (4).

Horsfall, O.I., Uko, E.D., Tamunobereton-ari, I., 2013. Comparative analysis of sonic and neutron-density logs for porosity determination in the south-eastern Niger Delta Basin, Nigeria. Am. J. Sci. Ind. Res. 4 (3), 261–271.

Ingram, G.M., Urai, J.L., Naylor, M.A., 1997. Sealing processes and top seal assessment. Nor. Pet. Soc. (NPF) Spec. Publ. 7, 165–174.

Kulke, H., 1995. Nigeria. In: Kulke, H. (Ed.), Regional Petroleum Geology of the World. Part II: Africa, America, Australia and Antarctica. Gebrüder Borntraeger, Berlin, pp. 143–172.

Landmark Graphics Corporation, 2008. Discovery T^{M} Halliburton. GeoGraphix Project Explorer. Version 5000. 0. 0. 0.

Lawal, Wasiu, 2015. Fault seal analysis a method to reduce uncertainty in hydrocarbon exploration: case study of moyo field Niger Delta basin. In: A Paper Presented at Dharmattan Nigeria Limited General Meeting, May 27, 2015.

Maunde, A., Henry, U., Raji, A.S., Haruna, I.V., 2013. Fault Seal analysis: a regional calibration Nile Delta, Egypt. Int. Res. J. Geol. Min. 3 (5), 190–194.

Muslime, B.M., Moses, A.O., 2011. Reservoir characterization and paleo-stratigraphic imaging over Okari field, Niger Delta using neutral networks. Lead. Edge 1 (6), 650–655.

Oil and Gas, 2015. Oil and Gas Page. www.nipc.gov.ng/oil&gaspage.html. Retrived on 5th October, 2015.

Oniyangi, S.M., 2008. Fault Seal Analysis of 'Ramat' Field in Niger Delta, Nigeria (Unpublished Master of Applied Geophysics Thesis). University of Lagos, Nigeria.

Owoyemi, A.O.D., 2004. Sequence Stratigraphy of Niger Delta, Delta Field (Offshore Nigeria. M.Sc. Thesis). Texas A & M University, USA.

Oyedele, K.F., Ogagarue, D.O., Mohammed, D.U., 2013. Integration of 3D seismic and well log Data in the optimal reservoir charaterization of EMI field, offshore Niger Delta oil province, Nigeria. Am. J. Sci. Ind. Res. 4 (1), 11–21.

Oyeyemi, K.D., Aizebeokhai, A.P., 2015. Hydrocarbon trapping mechanism and petrophysical analysis of afam field, offshore Nigeria. Int. J. Phys. Sci. 10 (7), 222–238.

Rider, M., 2000. The Geological Interpretation of Well Logs, second ed. Whittles Publishing, pp. 67–90. Chapter 7: Caithness Scotland.

Sahoo, Tuser Ranjan, Nayak, Sankar, Senapati, Shaktimatta, Singh Yogendra, N., 2010. fault seal analysis: a method to reduce uncertainty in hydrocarbon exploration. In: Case Study: Northern Part of Cambay Basin. 8th Biennial International Conference and Exposition on Petroleum Geophysics, pp. 1–9.

Schlumberger, 1989. Log Interpretation, Principle and Application. Schlumberger Wireline and Testing, Houston Texas, pp. 21–89.

Schowalter, T.T., 1979. Mechanics of secondary hydrocarbon migration and entrapment. Am. Assoc. Pet. Geol. Bull. 63, 723–760.

Short, K.C., Stauble, A.J., 1967. Outline of geology of Niger Delta. AAPG Bull. 51, 761–779.

Watts, N.L., 1987. Theoretical aspects of cap-rock and fault seals for single-and two-phase hydrocarbon columns. Mar. Pet. Geol. 4, 274–307.

Yielding, G., 2002. Shale gouge ratio-calibration by geohistory. In: Koestler, A.G., Hunsdale, R. (Eds.), Hydrocarbon Seal Quantification, vol. 11. Norwegian Petroleum Society Special Publication, pp. 109–125.

Yielding, G., Freeman, B., Needham, D.T., 1997. Quantitative fault seal prediction. AAPG Bull. 81, 987–917.